Journal of Infrastructure, Policy and Development 2025, 9(1), 10173.
https://doi.org/10.24294/jipd10173

Article

Preliminary approach of oil spill model: A hindcasting with in situ data and numerical model in Balikpapan Bay, Indonesia

Andri Purwandani[1], Wiwin Ambarwulan[2], Aninda W. Rudiastuti[1], I Wayan Nurjaya[3], Widiatmaka Widiatmaka[4,*], Rahmat Abbas[5], Yudi Anantasena[6], Djoko Nugroho[7], Yusuf Surachman Djajadihardja[7], Ety Parwati[8], Maryani Hartuti[8], Syarif Budhiman[8]

[1] Research Center for Conservation of Marine and Inland Water Resources, National Research and Innovation Agency (BRIN), Cibinong 16911, Indonesia
[2] Research Center for Limnology and Water Resources, National Research and Innovation Agency (BRIN), Cibinong 16911, Indonesia
[3] Faculty of Fisheries, IPB University, Bogor 16680, Indonesia
[4] Faculty of Agriculture, IPB University, Bogor 16680, Indonesia
[5] Department of Natural Resource and Environmental Science, Al Muslim University, Bekasi 17510, Indonesia
[6] Research Center for Mining Technology, National Research and Innovation Agency (BRIN), Lampung 35361, Indonesia
[7] Research Center for Geological Disaster, National Research and Innovation Agency (BRIN), Bandung 40135, Indonesia
[8] Research Center for Geoinformatics, National Research and Innovation Agency (BRIN), Bandung 40135, Indonesia
*** Corresponding author:** Widiatmaka Widiatmaka, widiatmaka@apps.ipb.ac.id

CITATION

Purwandani A, Ambarwulan W, Rudiastuti AW, et al. (2025). Preliminary approach of oil spill model: A hindcasting with in situ data and numerical model in Balikpapan Bay, Indonesia. Journal of Infrastructure, Policy and Development. 9(1): 10173. https://doi.org/10.24294/jipd10173

ARTICLE INFO

Received: 7 November 2024
Accepted: 19 December 2024
Available online: 7 January 2025

Abstract: Oil spills (OS) in waters can have major consequences for the ecosystem and adjacent natural resources. Therefore, recognizing the OS spread pattern is crucial for supporting decision-making in disaster management. On 31 March 2018, an OS occurred in Balikpapan Bay, Indonesia, due to a ship's anchor rupturing a seafloor crude oil petroleum pipe. The purpose of this study is to investigate the propagation of crude OS using coupled three-dimensional (3D) model from DHI MIKE software and remote sensing data from Sentinel-1 SAR (Synthetic Aperture Radar). MIKE3 FM predicts and simulates the 3D sea circulation, while MIKE OS models the path of oil's fate concentration. The OS model could identify the temporal and spatial distribution of OS concentration in subsurface layers. To validate the model, in situ observations were made of oil stranded on the shore. On 1 April 2018, at 21:50 UTC, Sentinel-1 SAR detected an OS on the sea surface covering 203.40 km^2. The OS model measures 137.52 km^2. Both methods resulted in a synergistic OS exposure of 314.23 km^2. Wind dominantly influenced the OS propagation on the sea surface, as detected by the SAR image, while tidal currents primarily affected the oil movement within the subsurface simulated by the OS model. Thus, the two approaches underscored the importance of synergizing the DHI MIKE model with remote sensing data to comprehensively understand OS distribution in semi-enclosed waters like Balikpapan Bay detected by SAR.

Keywords: 3D hydrodynamic; MIKE3 FM; MIKE OS; oil fate; oil slick; oil stranding; Sentinel-1 SAR

1. Introduction

The oceans are vital repositories of biodiversity and play a substantial role in regulating the global climate by absorbing greenhouse gases. They also support the supply of food and energy (Guan et al., 2019). The importance of oceans extends to oil and gas exploration activities, which enhance the economic sustainability of a country. However, human activities often jeopardize marine resources as they relate to pollution and degradation, resulting in a decline in the performance of ecosystems services (Weiskopf et al., 2020). Offshore oil exploitation activities are often closely

associated with oil spill (OS) accidents, which threaten the marine ecosystem and human life, increase marine and coastal pollution activities, and cause substantial economic losses (Apiratikul et al., 2020; Hong et al., 2020). Several occurrences such as ships accidents (Nixon and Michel, 2018), pipeline leaks (Wang et al., 2013), illegal fuel dumping, rig leaks, malfunctioning platforms, and well explosions (Daly et al., 2021) are the leading causes of OS accidents.

The global incidence of OS has increased interest in modelling and monitoring OS distribution and analyzing its ecological impact (Bejarano et al., 2023). Some researchers have studied the OS distribution using satellite data and numerical models (Cheng et al., 2024; Fingas and Brown, 2014; Li et al., 2023). Among these methods, Sentinel-1 SAR (Synthetic Aperture Radar) was widely used for OS mapping in various locations globally (Melillos and Hadjimitsis, 2021; Prastyani and Basith, 2018; Rajendran, Vethamony, Sadooni, Al-Kuwari, Al-Khayat, Seegobin, et al., 2021). However, it should be noted that Sentinel-1 SAR is limited to detecting oil spills (OS) on the water surface (Fingas and Brown, 2017). There remains a gap in understanding the full distribution of OS throughout the water column and down to the seabed, as remote sensing data alone cannot provide insights into subsurface oil dynamics.

Numerical models have increasingly become vigorous tools in monitoring and forecasting oil dispersion, as they enable simulations of oil thickness, concentration, and trajectory predictions. Over recent decades, OS models have employed the Lagrangian oil particle methodology, which serves as a primary method for forecasting OS trajectories (Liu et al., 2022). Notably, the Lagrangian OS transport model has been utilized in various applications, including OSCAR/Oil Spill Contingency and Response (Barreto et al., 2021), NOAA's GNOME/General Operational Oil Modeling Environment (Gurumoorthi et al., 2021), MOSM/Marine Oil Spill Management (Huang et al., 2020), and the MIKE21/3 Spill Analysis (SA) module and ECOLAB model (Gao et al., 2022).

DHI's MIKE modeler software is frequently used for two-dimensional (2D) or three-dimensional (3D) modeling phenomena in many environments. Liu et al. (2022) demonstrated that the simulated tide levels, tidal current speeds, and directions using MIKE21 align closely with data measured in the Chengdao oil field. Similarly, Hidayat et al. (2021) combined the TUNAMI and MIKE21 HD with the SA model to study OS in Cilacap, Indonesia. The MIKE model suite, including MIKE21 and MIKE3, is frequently recommended for OS modeling due to its ability to couple hydrodynamic and spill fate modules, such as the MIKE OS module, which simulates oil transport, dispersion, and degradation processes. While specific endorsements by the International Maritime Organization (IMO) or the International Tanker Owners Pollution Federation (ITOPF) may vary based on case-specific needs, MIKE is widely used in academia and industry and adheres to best practices for modeling OS scenarios. Its integration of hydrodynamics, oil fate modeling, and environmental impact assessment makes it a valuable tool for addressing the challenges of OS mitigation and planning. For rapid response to OS, trajectory models such as GNOME are commonly used to predict oil movement immediately following an incident. However, for detailed post-spill assessments, fate models are often preferred as they account for processes such as dispersion, evaporation, emulsification, and degradation. The MIKE

suite, including the MIKE OS module, stands out for its comprehensive fate modeling capabilities, offering a more detailed numerical analysis compared to other tools like MOHID, GNOME, or OSCAR, which primarily focus on trajectory modeling. This makes MIKE an invaluable tool for addressing the broader environmental impacts of OS and planning effective mitigation strategies.

In Indonesian waters, several significant OS incidents have occurred, such as the Timor Sea spill in East Nusa Tenggara on 21 August 2009 (Spies et al., 2017), and the spill near Bintan Island due to illegal tank cleanings (Sulma et al., 2019). One of the most tragic incidents in the past decade was the Balikpapan Bay spill in East Kalimantan, Indonesia, on 31 March 2018, causing severe health and economic impacts while threatening local ecosystems. Despite previous research, such as the work by (Prastyani and Basith, 2018) using Sentinel-1 SAR imagery, comprehensive modelling that covers OS distribution on the surface, water column, and seabed in Balikpapan Bay remains unexplored.

Building on the existing research and identified gaps, this study aims to map the distribution of the crude OS in Balikpapan Bay, Indonesia, using numerical modelling and remote sensing approach. Specifically, the coupled model using MIKE3 Flow Model (FM) and MIKE OS will be employed to simulate the distribution of the OS from the water column to the seabed surface. Additionally, Sentinel-1 SAR imagery will be utilized to capture the surface distribution of the OS. This integrated approach addresses the limitations of surface-only detection by synergizing it with subsurface modeling. By doing so, it provides a comprehensive view of OS dynamics across the entire water column in complex marine environments like Balikpapan Bay, offering critical insights that can aid in effective disaster mitigation and environmental management.

2. Materials and methods

2.1. Study area

Balikpapan Bay is a semi-enclosed water body located in East Kalimantan Province, Indonesia, as shown in **Figure 1**. The bay has a depth range of 2 to 58 m, with a maximum depth of 58 m. The seabed is composed of a mix of sediment types, including muddy, sandy-mud, and coarse sediments. The coastline of this region hosts the largest oil refinery and various other industries along the eastern coast. Over the past decade, the dense mangrove coverage along the entire coast has played a significant role in supporting the local coastal communities by providing resources such as fish, wood, and other materials essential for their livelihoods (Lahjie et al., 2019). The bay experiences a meso-tidal regime, with a tidal range of approximately 3 m, and the water currents are influenced by the dynamic exchange between mangrove waterways and the open waters (Muin et al., 2022). These physical and hydrodynamic characteristics make Balikpapan Bay a highly dynamic environment, with complex interactions between human activities, natural processes, and ecological systems, which are crucial to consider in oil spill modeling and mitigation efforts.

In **Figure 1**, several points observations were made for field modeling and validation purposes. Two tidal observation stations (TD1 and TD2), one ADCP (Acoustic Doopler Current Profiler) station, and sediment observations points for oil

stranding measurements were established along the coast (dots at C1-C4). Meanwhile, transects L1-L2, L3-L4, P0-P1, and P0-P2 are virtual lines that will be used to show the distribution profile of crude oil amount moving in and out of the bay, as modeled against the 3D current circulation pattern (in results and discussion section). Wind data was taken from the closest ECMWF grid to the model domain, which is located on the coast near the Acoustic Doppler Current Profiler (ADCP) point (**Figure 1**, red triangle). Meanwhile, the location of the crude OS near the seabed (at a depth of 28 m depth) was identified at the point P0 (geographically located at 01°14′42.1″ S and 116°47′16.2″ E. The spill occurred on 30 March 2018, at 3:30 pm (UTC) and continued until 3:10 am (UTC) on 1 April 2018.

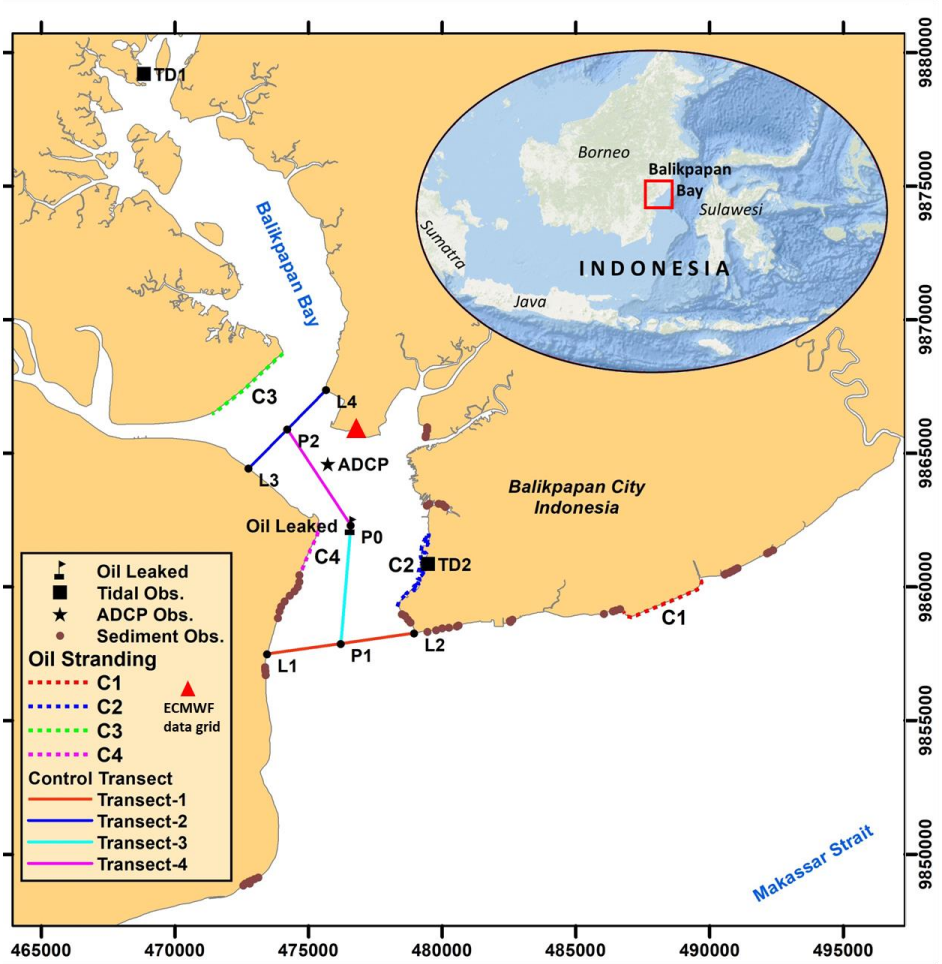

Figure 1. Study site at Balikpapan Bay, Indonesia.

Note: The map used the UTM50S projected coordinate system.

2.2. Model setting

This study utilized two approaches with specific data requirements for effective processing. The first approach was numerical modeling using the MIKE3 FM Hydrodynamic (DHI, 2013a) coupled with MIKE OS Module (DHI, 2013b) to simulate the subsurface distribution of the OS, from the water column to the seabed. The model input included an OS volume of 2402.97 m^3, equivalent to 15,114.2 barrels, as officially reported by Pertamina RU V Balikpapan. The modeling process relied on a comprehensive set of parameters and datasets summarized in Supplementary **Table**

S1. The completeness of input data—whether primary data, supporting datasets, or parameterized inputs—is crucial for producing reliable outputs.

Critical information such as oil characteristics, model assumptions, and secondary forcing factors were detailed in Supplementary **Tables S2–S4**, respectively, providing additional context and precision for the model. These parameters were carefully selected to reflect the physical characteristics and hydrodynamic conditions of Balikpapan Bay, ensuring the model accurately captured the spill dynamics. Since in this study we use the MIKE3 FM Module for the hydrodynamics model coupled with the MIKE OS Module, here and after, the OS model in this paper refers to this definition. Likewise, the use of the term subsurface layer reflects the depth-integrated from the water column layer to the seabed surface.

The simulation was conducted over 9 days, from 17 May to 25 May 2018. The bathymetric data were divided into a limited mesh of 223,679 triangular elements with ten vertical layers. The spatial pattern design used a finite element (triangular element) type (Supplementary **Figure S1**), where each node at the intersection of these elements became a calculation point, with varying resolution depending on the size of each triangular element. The model produced key outputs such as flux in the x-y direction, zonal and meridional current components, and changes in water level over time.

Additionally, model accounted for the vertical dispersion of oil, using numerical calculations to simulate oil resuspension. In constructing numerical model, several aspects were considered, including the physical properties related to changes in viscosity and density, oil clean up (oil booms and dispersants), and the calculation of stranded oil. The model outputs include the total area affected by the crude OS and the amount of crude oil in different parts of the water column.

The spatial resolution used in the modelling, as presented in Supplementary Files (**Figure S1**), was automatically generated by MIKE through finite elements of varying sizes, resulting in no single consistent spatial resolution across all elements. The temporal resolution for the time step ranged from 0.01 to 30 s, adjusted to ensure compliance with the Courant number requirement (< 0.8). MIKE generated model outputs at a temporal resolution of 10 min. The MIKE3 FM model solves three-dimensional, time-dependent conservation equations for mass and momentum using the Reynolds-Averaged Navier-Stokes framework. It applies an explicit finite difference method and adheres to the Courant-Friedrichs-Lewy (CFL) stability criterion (De Padova et al., 2017). The dataset for the modeling included wind data (Supplementary **Table S1**) from ERA Interim, with a temporal resolution of 6 h, representing one data point per model domain. The data spanned one month (30 March to 29 April 2018) following the OS event. The research workflow, illustrated in **Figure 2**, was divided into three stages: (i) hydrodynamic modeling and validation; (ii) OS modeling and validation; and (iii) oil slick mapping using Sentinel-1 SAR imagery.

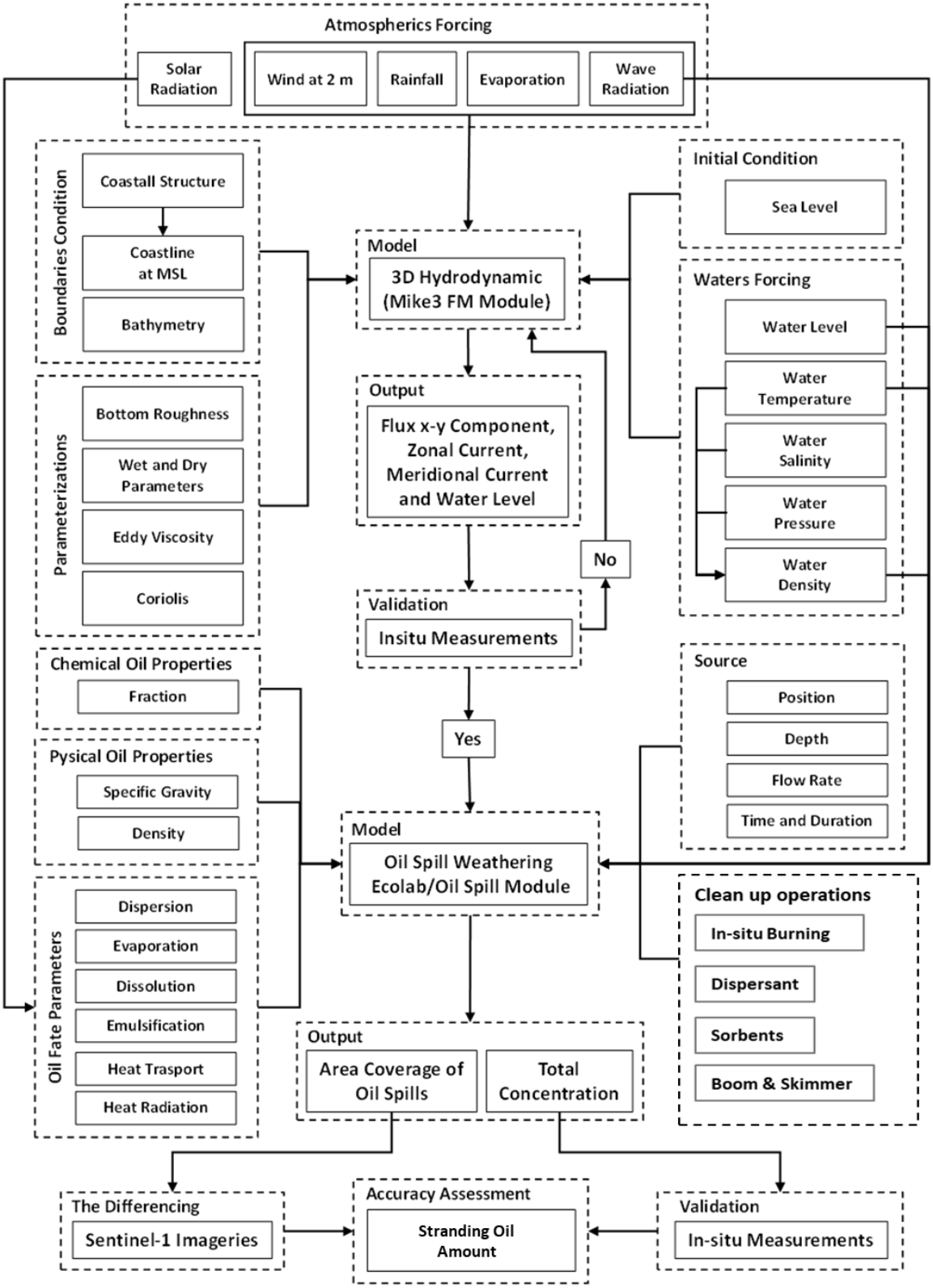

Figure 2. Research flowchart.

2.3. In-situ measurement and validation

Field observations were conducted from 16 to 25 May 2018; several in-situ parameters were collected to validate the model, including hydrodynamic data such as

currents, tides, and sediment samples (for oil stranded on coastal sediments or trapped in coastal sediment grains). The distribution of in-situ observation stations is shown in **Figure 1**. Balikpapan Bay, known for its dynamic hydrodynamics, is prone to fluctuations in pollution concentrations, as tidal movements and currents can carry contaminants in and out of the bay.

The design and spacing of these measurement stations were meticulously planned to account for the unique physical characteristics and hydrodynamics of Balikpapan Bay. For the hydrodynamic modeling, two Tide Gauges were installed. One was placed in the inner bay (TD1), where the influence of tidal wave propagation from the sea is minimal, while the other was positioned at the bay's mouth (TD2), where tidal wave propagation from the sea is more significant. These installations were essential for validating the model's water level outputs. An ADCP was deployed in the center of the bay to measure currents, as this area is expected to have unique and complex circulation patterns due to the convergence of large rivers from the north (Riko and Wain Rivers), combined with the influence of the Makassar Strait. For validating the crude OS distribution model oil stranding analysis on coastal sediments (C1-C4 in **Figure 1**) were carried out.

A total of 56 sediment samples were systematically collected from 12 observation points along the coastal area (C1-C4), with each sample representing sediment depths of 0–30 cm, 30–60 cm, 60–90 cm, and 90–120 cm. This stratified sampling approach was designed to capture the oil distribution across different sediment layers, assuming consistent sediment density across these depths. The C1-C4 locations were selected to reflect the diverse hydrodynamic conditions that affect oil concentration and movement, thus providing an understanding of the distribution of stranded oil. Location C1 represents an area exposed to strong winds and high wave energy, while location C2 is a built-up coastal area with relatively deep waters, strong currents, and lower wave energy. Location C3, conversely, is characterized by low current velocities and wave energy with gently sloping coastlines. Lastly, location C4 in the western part of Balikpapan Bay reflects more natural conditions, with the gentlest beach slopes but relatively high current velocities. The choice of measuring stranded oil in coastal sediments was based on its ability to represent oil content across different layers of the water column (surface to bottom) in the intertidal zone, providing a more comprehensive picture than surface water measurements alone, which only capture oil concentrations in the top layer. To further picture the horizontal distribution and movement of crude oil amount in the subsurface layers, virtual transects in **Figure 1** were designed to represent the cross-sectional movement of oil across the bay (L1-L2 and L3-L4), while Transects 3 (P0-P1) and 4 (P0-P4) focused on the longitudinal movement of oil along the bay.

For validation, the OS model was compared with the in-situ stranded oil, consisting of 56 sediment samples on the coast. Meanwhile, the sediments used were expected to have the same density as the surrounding sediment. Suspended and sedimented oil amount expressed in mg/L were converted to mg/kg using the specific gravity of each sample, followed by grouping by similarity. Consequently, 19 sediment density values, approximately 2640 mg/kg samples were selected to validate the OS model.

The modeling of water circulation dynamics using the MIKE3 FM HD Module (DHI, 2013a) aimed to understand how oil entered the Balikpapan Bay water system and to predict the movement and spread of OS. This stage involved applying the MIKE3 FM Module for the hydrodynamic model, which included external forcing, boundary conditions, model parameterization, and spatial grid design. The atmospheric forcing process included key parameters such as solar radiation, wind at 2 m, rain, evaporation, and wave radiation. These atmospheric factors influenced overall water dynamics and were crucial in determining how oil spread during a spill. As the oil spilled in the water bay, thus the wind and tides were used as boundary conditions (Zu and Gan, 2009). Additionally, boundary conditions such as coastal structures, coastline at mean sea level (MSL), and bathymetry data were incorporated into the model (DHI, 2014a). This hydrodynamic model served as the input foundation for OS modeling using the MIKE OS Module. In-situ measurements of water level (tides) and currents were used to validate the model data over a 9-day period, from 17 May to 25 May 2018. Also, for validation purpose, the zonal and meridional current components is on vertically averaged value.

The MIKE3 FM Module for the hydrodynamic model was coupled with the MIKE OS Module to model the fate and distribution of the crude OS in Balikpapan Bay. Once the hydrodynamics are modelled, the OS behavior is simulated using a MIKE OS Module/ECO Lab (DHI, 2013b) with the weathering algorithm (DHI, 2014a). The model used numerical equations to simulate the physical-chemical-biological processes of the oil (DHI, 2014b), such as specific gravity and density, and incorporates critical processes that affect the oil's behavior in the water, including dispersion, evaporation, dissolution, emulsification, and heat transport (Motorin et al., 2022). These factors were intricately associated with spillage, physical and chemical properties, oil thickness, oceanographic, and meteorological conditions (Liu and Callies, 2019).

2.4. Oil spill distribution based on Sentinel-1 SAR

To illustrate the distribution of the OS on the surface waters of Balikpapan Bay, the method described by (Prastyani and Basith, 2018) was re-processed using Sentinel-1 SAR imagery acquired on 1 April 2018. Their approach utilized the automatic OS Detection tool in the Sentinel Application Platform (SNAP), which applies the Adaptive Threshold Method for detecting oil slicks. The pre-processing steps included radiometric and geometric calibration, speckle filtering, and wind estimation using CMOD5.N (Rana et al., 2019). The detection process involved identifying dark patches in the SAR imagery, extracting features such as shape and texture, and classifying oil slicks to differentiate them from look-alikes such as natural slicks or calm water (Rajendran et al., 2021). The dark area detection process identifies regions of reduced backscatter in SAR imagery, which typically appear as dark patches. This is crucial for isolating potential oil slicks on the water surface. Feature extraction involves analyzing these dark areas to derive characteristics such as shape, size, and texture, which help differentiate oil slicks from "look-alikes" (e.g., natural slicks, algae, or calm water). The oil/look-alike classification step then uses these extracted features to classify detected dark areas, ensuring that only true OS are identified while

minimizing false positives. This sequence of steps is essential for accurate OS detection and mapping.

The resulting map (**Figure 3**) shows the OS distribution derived from Sentinel-1 imagery, highlighting distinct dark patches that represent oil slicks concentrated along the southern parts of Balikpapan Bay, extending toward the open sea. The lighter areas in the northern section correspond to unaffected land and riverine zones. These results align with the dynamic hydrodynamic processes in the bay, where tidal and current-driven forces influence oil accumulation and dispersion.

This map provides a visual reference for surface OS patterns and serves as a comparison for the results of the MIKE OS modelling presented in Chapter 3, which explores the behavior of OS distribution within the water column and its differences from surface patterns.

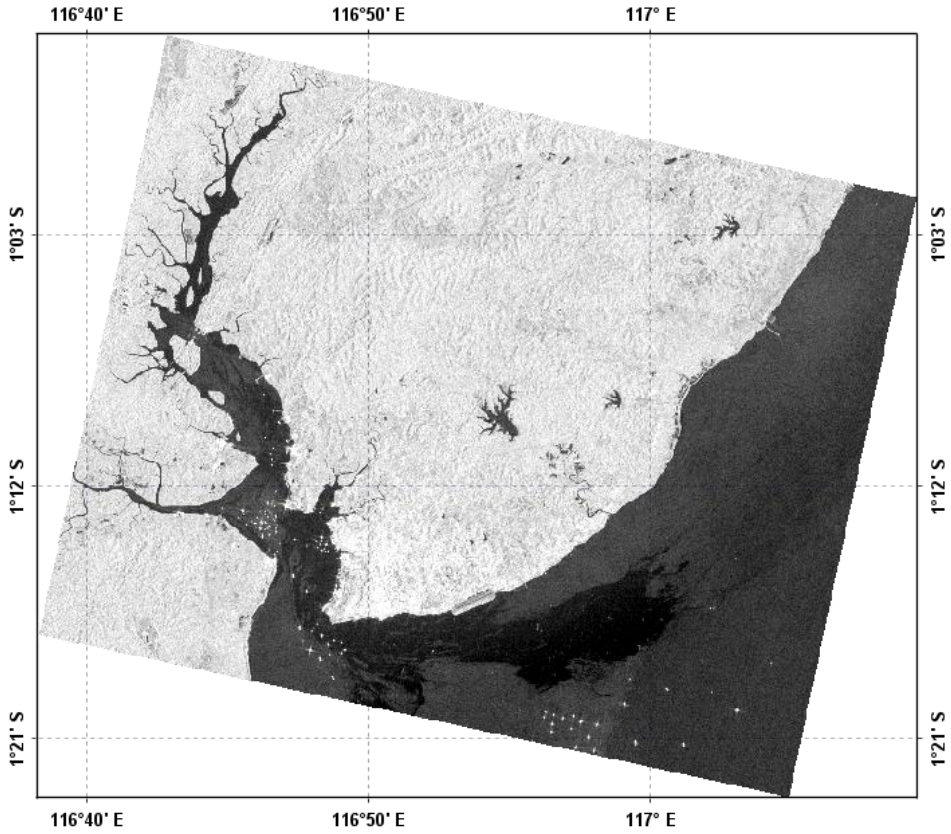

Figure 3. Sentinel-1 SAR image (1 April 2018) showing OS distribution (dark feature) in the surface water of Balikpapan Bay.

3. Results and discussion

3.1. Hydrodynamic model validation and current circulation analysis

Water level data from in-situ observations (see Supplementary **Table S5**) along 9 days from 17–25 May 2018 on TD1 and TD2 stations (**Figure 1**) in Balikpapan Bay revealed a semi-diurnal mixed tide. Hydrodynamic model data of water level compared to in-situ data was shown in **Figure 4** for both observation stations. The hydrodynamic model validation was performed using water level and current data

collected at two Tide Gauge stations (TD1 and TD2) and an ADCP station in Balikpapan Bay during 17–25 May 2018. The modeled water levels were compared to in-situ measurements, showing strong agreement with an R^2 of 0.92 at TD1 and 0.88 at TD2, and RMSE values of 0.18 m and 0.22 m, respectively (**Figure 4a**,**b**). These results indicate the reliability of the MIKE3 FM model in simulating tidal dynamics in the bay.

The comparison between simulated currents from MIKE3 FM Hydrodynamic model with the currents measured in ADCP station (see **Figure 1**) depicted in **Figure 4c**. The current observations data and model validation conducted at all depth layers (depth-integrated) were presented as zonal and meridional current components. The plot in **Figure 4c** indicated that the hydrodynamic model was performing well in simulating the general flow pattern of the water currents. The direction of the currents between the model and in-situ data were aligning moved to the north-south direction (meridional component). The condition indicated that tides predominantly influenced the circulation of currents in Balikpapan Bay. A bias was observed in the zonal component (west-east) current speed of 0 –0.15 m/s and the highest current speed in the meridional direction (north) of 0.48 m/s. According to model, the highest current speed was 0.54 m/s with a bias of 0.06 m/s. The meridional (south) current component from in-situ observations was obtained at 0.64 m/s, while model output was 0.50 m/s. These conditions indicated that the in-situ observations results were more dominated by the water mass movement out of the bay compared to model output. This finding along with Liu et al. (2022) who used MIKE21 FM at the Chengdao oil field in China and found that the height, speed, and direction were consistent with the measured data. Since the model was able to simulate the observed current dynamics with relatively high accuracy, the wind will be discussed in the following section.

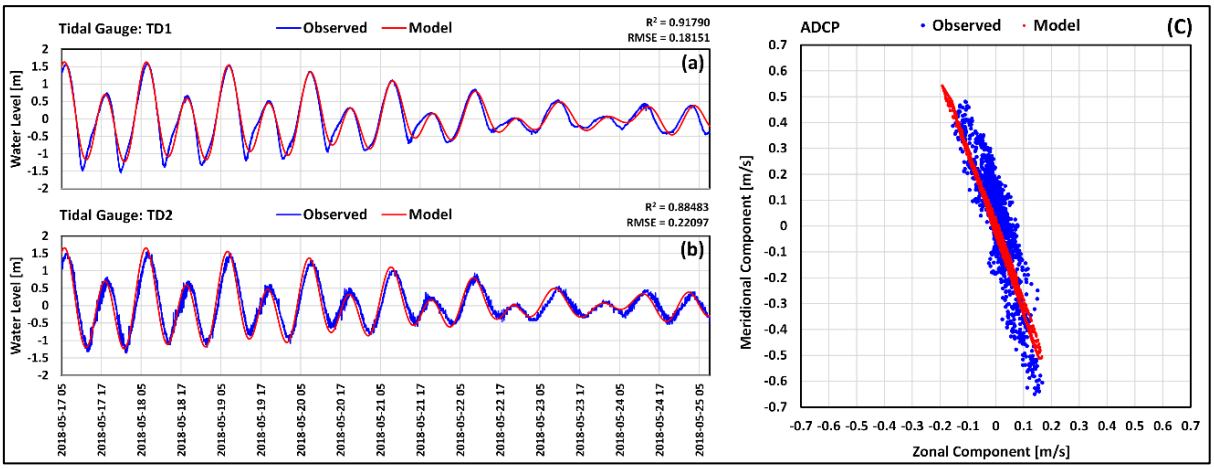

Figure 4. The comparison between time series of observed (blue line) and simulated (red line) of WL at TD1 (**a**) and TD2 (**b**).

Note: The zonal and meridional current components (vertically averaged) from the Hydrodynamic model and in-situ observations **(c)**.

The hydrodynamic model incorporates several model parameters, including morphology (bathymetry profile, coast, and bottom roughness), water properties (water column density), and atmospheric conditions (solar radiation, wind, rainfall, evaporation, and wave radiation). As indicated by (French-McCay et al., 2021; Khoi

et al., 2023) the main factors influencing current circulation include tides, sea surface winds, and water column density. The current vectors from the hydrodynamic model of Balikpapan Bay, averaged across depth-integrated at different tidal phases, presented in **Figure 5**. Current circulation patterns simulated by the hydrodynamic model (**Figure 5**) highlights tidal influences. For high tide and low tide scenarios, the current directions and magnitudes differ significantly. At high tide, water flows inward, with stronger currents observed near the bay's entrance, whereas during low tide, water flows outward, driven by the tidal elevation gradient. The current velocity variations reflect the bathymetry and the bay's semi-enclosed morphology. To enhance visibility, surface elevation in **Figure 5** should be plotted as isolines or omitted, as tidal reproduction accuracy is already demonstrated in **Figure 4**. Wind data shown in **Figure 5e** indicates predominant directions from the northeast and northwest, but the location of wind measurements (inside or outside the bay) remains unclear. Considering the potential impact of local orography on wind dynamics, additional wind data both inside and outside the bay would improve the accuracy of current circulation and OS trajectory simulations. Furthermore, the coastal currents outside the bay, which were not accounted for in this study, may significantly influence the OS's movement, particularly in the Makassar Strait.

In **Figure 5a**, Phase A at 11:05 AM UTC, the surface elevation is relatively high, particularly in the northern part of the bay and near the coastline, indicating an incoming tide or high-water event. The current vectors are oriented toward the northwest, suggesting that the water is being pushed out of Balikpapan Bay towards the open sea. The variation in bathymetry on the western side, which is shallower compared to the eastern side, affects the difference in current velocities on both sides of the bay. Towards **Figure 5b**, Phase B at 02:00 PM UTC, there is a transition to a lower surface elevation, closer to the mean water level. Higher current velocities are identified in the middle of the bay (0.61–0.82 m/s). The current vectors point outward, indicating that water is still flowing out as part of the outgoing tide cycle. This phenomenon occurs because the sea level in the open water has reached its lowest ebb.

In **Figure 5c**, entering Phase C at 04:40 PM UTC, the surface elevation continues to drop, particularly in the northern and central parts of the bay. The current flow is stronger near the northern outlet, with the direction continuing to flow out of the bay, further signaling an ebb tide. Finally, move to **Figure 5d**, Phase D at 08:15 PM UTC, a high-water event is depicted, with high surface elevations in the northern part of the bay, indicating water flowing into the bay during a flood tide. The current direction shifts inward, with maximum velocities greater than those in other tidal phases. After Phase D, the water mass circulation cycle returns to Phase A.

Figure 5e presents a wind rose diagram showing the wind speed distribution during the simulation period. Most wind speeds fall below 2.5 m/s and predominantly blow from the northeast and northwest directions. However, the relatively low wind speeds suggest that wind had a limited impact on surface currents during this period, as most of the wind speeds remained below 2.5 m/s, with only a small percentage exceeding 3.0 m/s.

From each phase condition, it can be inferred that the hydrodynamic model effectively captures the primary driver of current circulation patterns in Balikpapan Bay, which is the difference in tidal forces. The model shows clear inflows during

flood tides and outflows during ebb tides. Wind, although present, played a minor role in influencing surface currents due to the relatively low wind speeds during the simulation period. The model results provide a clear comprehension of how tidal forces govern water movement in and out of the bay, which has important implications for the transport and dispersion of materials such as OS.

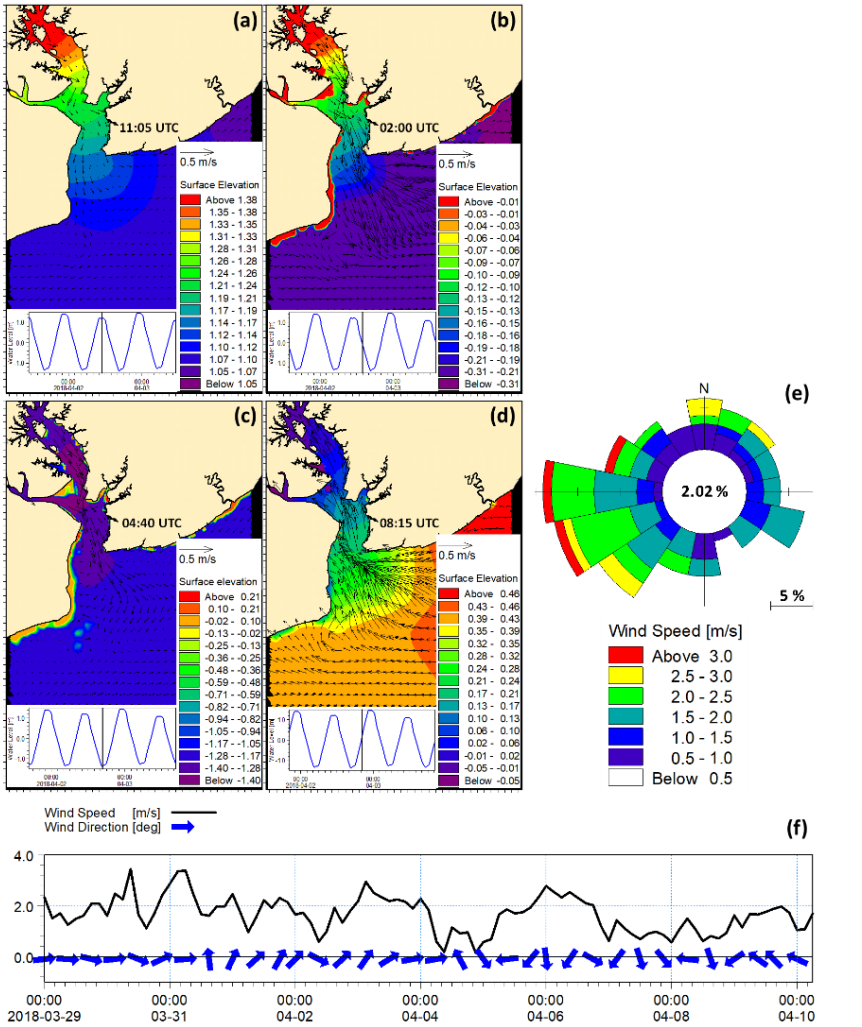

Figure 5. The average current circulation at different depth layers is shown for (**a**) Phase A; (**b**) Phase B; (**c**) Phase C; and (**d**) Phase D. Additionally; (**e**) depicts wind roses from 00:00 UTC on 29 March to 01:00 UTC on 10 April 2018; and (**f**) presents the wind time series, where the black line represents current speed (m/s), and the blue arrows indicate current direction.

Note: The black vertical lines on the tidal/water level graphs in **Figures 4a–d** mark the tidal phases.

3.2. OS model and validation

The oil fate process was crucial in determining the extent of oil concentration volume at a particular location and time. Since the leakage source of the OS in Balikpapan Bay originated from a pipe on the seabed surface, the presence of oil was not only on the surface but also in the water column to the seabed surface. Consequently, understanding the distribution of OS necessitated the integration of hydrodynamic modeling to determine OS distribution in the subsurface layer (from the water column to the seabed surface). It is along with findings by French-McCay et

al. (2021) where the OS biodegradation and weathering processes in the Deepwater Horizon case resulted in ~41% evaporated, ~38% degraded, ~3% deposited at the bottom and the rest on the water surface.

Figure 6 illustrates the evolution of oil amount in the subsurface layer of Balikpapan Bay over time, observed on Days 1, 3, 5, 7, 9, and 10.5 following the crude oil spilled into the sea water. Each map shows the spatial distribution of oil amount (mg/L) across the bay. According to the tidal phase, the spilled oil spread outward from the bay due to tidal currents generated by differences in tidal phases between the waters inside and outside the bay. The graphs in **Figure 6** display water level fluctuations and oil amount trends across four transects (L1-L2, L3-L4, P0-P1, and P0-P2). The color scale represents the total oil amount in the subsurface layer, including dissolved oil, suspended oil, and oil degraded by biodegradation processes. The graphs alongside the maps provide insights into the tidal cycle and oil amount across different transects in each time simulation.

On Day 1, with a total leakage time of 35 h and 40 min (see Supplementary **Table S2**, 1200 m^3/h), high amount of crude oil were confined to areas near the spill source. The OS simulation showed rapid oil spreading inside the bay, extending 5.6 km toward the bay's interior and 12.8 km toward the open sea (southeast). The total area coverage of the OS modelled on Day 1 was approximately 98.96 km^2, with estimated oil amount of up to 800 mg/L at the bay entrance. Meanwhile, depth-integrated oil amount reached up to 2495 mg/L in the middle of the inner bay, higher than those observed outside. This phenomenon occurred due to the movement of water masses out of the bay at low tide (see water level on Day 1 in **Figure 6**). Along Transect 1, the highest oil amount was 4200 mg/L, while Transect 2 exhibited a maximum value of 2800 mg/L. Oil amount decreased from 6500 mg/L (P0) to 1500 mg/L (P1) along Transect 3, and a similar decreasing trend was observed along Transect 4, moving from the leakage site toward the inner bay.

On Day 3, the source of the OS was confined, and amount levels at each transect were higher compared to Day 1, indicating the movement of oil away from the source. The OS extended 19.7 km from the pipe leak source (indicated by the flag in **Figure 1**) into the open sea and 14.2 km into the bay, effectively doubling the exposed area to 225.37 km^2. According to **Figure 6**, on Day 3, the OS infiltrated coastal waters. The highest amount of 10,000 to 17,000 mg/L were observed on the west side of the bay, where the bathymetry was shallow and sloping. Meanwhile, OS amount ranged from 2200 to 5100 mg/L on the east side toward the estuary. The bathymetry profile led to a higher amount of oil stranded on the west coast, compared to the east with steeper coastal.

By analyzing the distance and distribution area modeled by the MIKE 3 OS Module in **Figure 6**, the OS model predicted the farthest distance toward the open sea was 21.2 km, 22.9 km, 23.5 km, and 23.8 km on the 5th, 7th, 9th, and 10.5th days, respectively, and the distance of the OS inward the bay reached 14.5 km, 14.8 km, 15.6 km, and 15.8 km, respectively. The area of Balikpapan Bay exposed to the OS increased gradually, reaching 348.24 km^2, 448.58 km^2, 512.72 km^2, and 546.98 km^2 on Days 5, 7, 9, and 10.5, respectively. According to the oil amount graphs for each simulation time (**Figure 6**), major shifts in oil amount were observed, increasing fivefold from Day 1 to Day 10.5. This indicated that more oil was deposited on the

seafloor and rolled onto the beaches, forming tar balls. Similarly, the dispersed and dissolved oil, manifesting as slicks and sheen, weathered, stranded, and accumulated on the shore. Oil amount in the central waters gradually decreased, and the OS in the water column to the seabed surface expanded further into the open sea.

3.3. Oil stranding

Small amounts of oil can persist for decades in the intertidal zones on the coarse sediment of the coast. It typically survives in forms such as tar mats or subsurface residues until environmental changes, such as storms or long-term erosion, alter the conditions that allow for continued biodegradation (Owens et al., 2008).

In this study, the OS modeling integrated the calculation of stranded oil using seabed roughness as a proxy to determine the presence of oil, whether it remains in the water, is temporarily stranded before returning to the water, or is carried directly to deeper waters. This process refers to the parameter of water depth, which is influenced by tidal heights (DHI, 2014a). Automatically, seabed roughness is considered in the modeling using MIKE3 FM software (DHI, 2013a), which calculates the depth-averaged velocity. If the velocity reaches zero due to high seabed roughness values and water depth approaches zero (during low tide), oil will become stranded on the coast.

The spatial distribution of the average oil amount (mg/kg) stranded in the intertidal zone of Balikpapan Bay during the modeling period is shown in **Figure 7**. This average represents the amount of oil amount trapped and stored in porous sediment grains, allowing oil to penetrate the sediment column. Generally, the amount of stranded oil is proportional to the size of the intertidal zone, which is influenced by a sloping bathymetric profile. The simulation results show that oil stranding accumulates along the western coast of Balikpapan Bay, where shallow waters (see the bathymetry inset in **Figure 7a**) and gently sloping beaches are found. Additionally, **Figure 7a** includes a graph showing oil stranding amount trends simulated along four coastal sections (C1, C2, C3, and C4) which represent model result in intertidal zone. The graph provides a detailed variation of oil stranding amount along four specific coastal transects. The x-axis represents the distance of 3 km perpendicular to the coastline. Detailed variations in the simulated oil stranding amount for each section are presented in Supplementary **Table S6**.

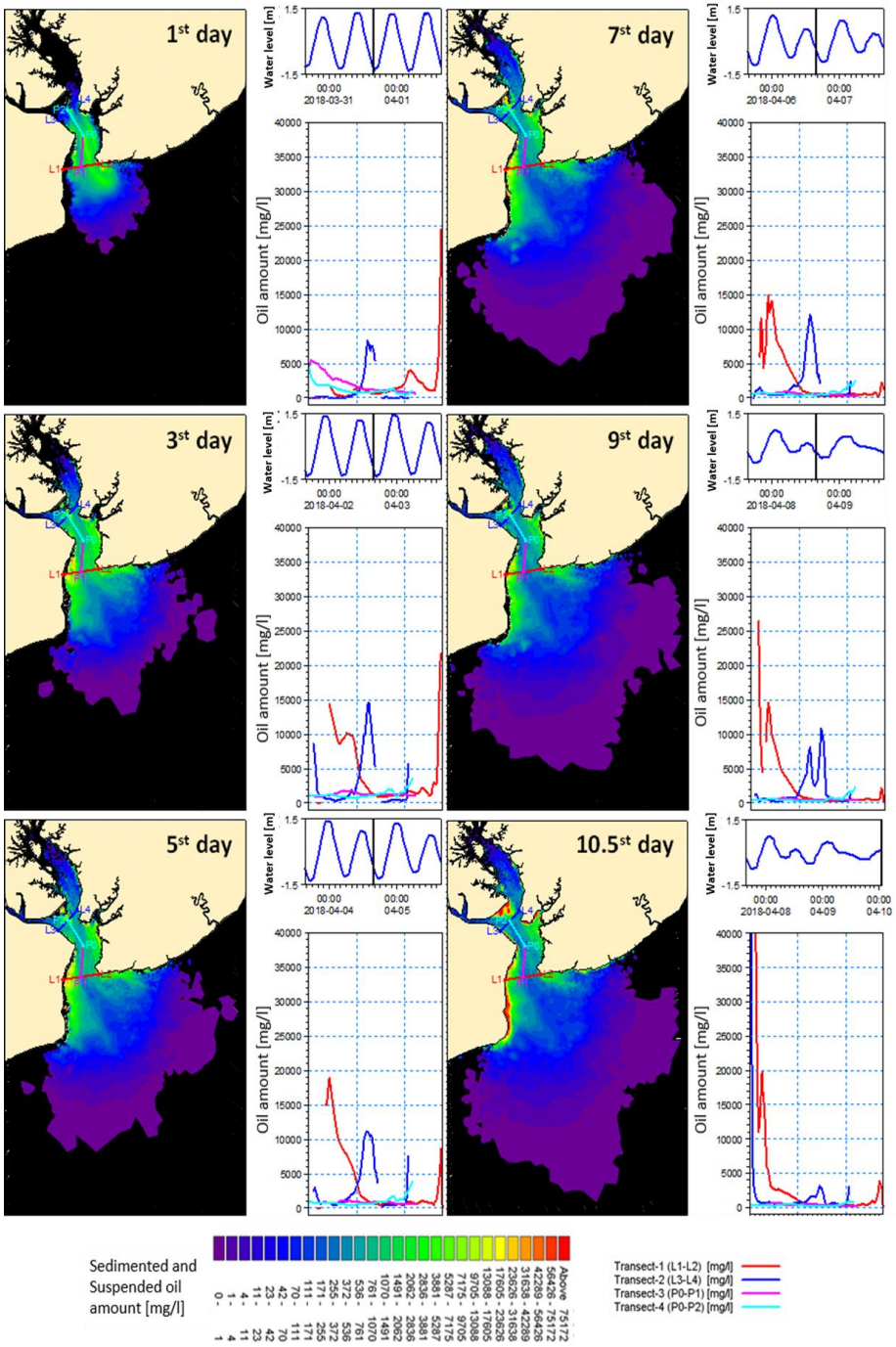

Figure 6. The OS distribution in the subsurface layer (depth-integrated from the water column to the seabed surface) was simulated using the MIKE 3 OS Module in Balikpapan Bay at 1, 3, 5, 7, 9, and 10.5 days. The graph next to the model illustrates the variation of oil amount (mg/L) in Transect-1 (L1-L2), Transect-2 (L3-L4), Transect-3 (P0-P1), and Transect-4 (P0-P2) on different simulation days.

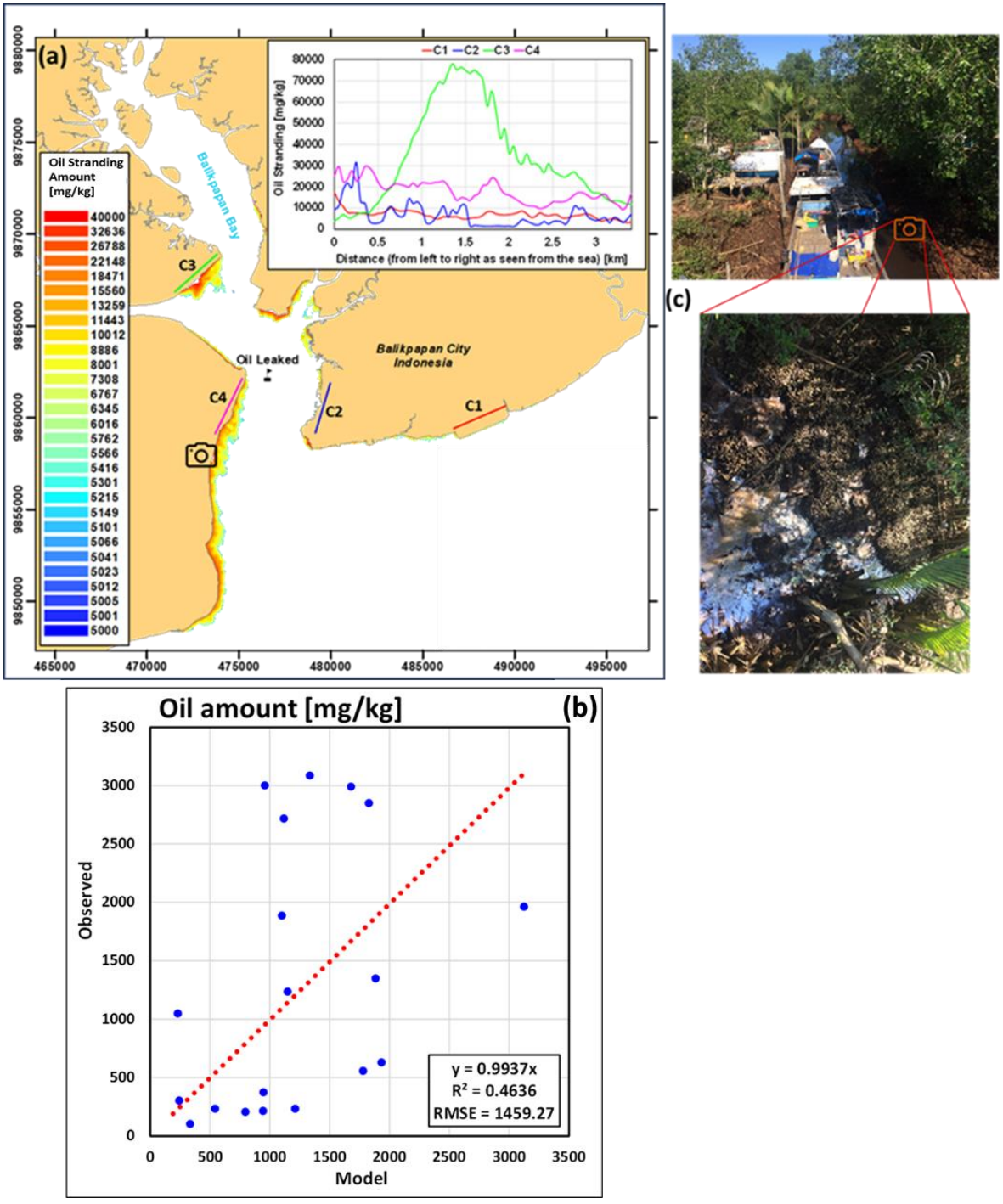

Figure 7. The spatial distribution of stranded oil amount (mg/kg) in the intertidal zone of Balikpapan Bay. The inset graph shows the stranded oil amount variation in the intertidal zone/coastal zone along a 3 km transect at C1, C2, C3, and C4 (**a**). The comparison between in-situ observed oil amount in sediments (**Figure 1**) in the intertidal zone and 3D OS modeling results (**b**). A photo of an OS taken along the edge of the Nenang River in Penajam-North Paser Regency, 458 m from the beach (indicated by the camera symbol on the map at a position 116°45′30.22″ E and 1°17′13.81″ S), was taken on 17 April 2018, 17 days after the oil leaked (**c**).

According to the data in Supplementary **Table S6**, the highest average oil stranding amount was found in Transect C3, while the lowest was in C2. Transect C3 exhibited the highest amount range because the current direction moved into the estuary, transporting water masses with high oil amount. In this location, the influence

of slow ocean currents diminished, accelerating oil deposition until it eventually became stranded. Since C3 is in the innermost part of the bay, the influence of waves was minimal. As a result, wave propagation due to wind friction was insufficient to erode stranded oil back into the water column. The OS model has this capability because it is coupled with MIKE3 FM (DHI, 2013a). Meanwhile, the second highest simulated oil amount was observed in Transect C4, which showed a relatively constant amount of stranded oil. This is likely due to its natural coastal environment, dense mangrove vegetation, and gently sloping shore conditions.

At Location C1 (see Section 2.3), an area exposed to strong winds and high wave energy, oil droplets formed below the surface oil layer. These oil droplets were quickly carried away in the direction of currents and winds moving eastward. On Transect C2, the coastal area, despite being built-up, had the potential to trap oil. However, based on the modeling results, Transect C2 showed minimal amount, likely due to the coastal structure's bathymetric profile, which allowed tidal currents to freely distribute oil out of the bay and minimize oil adhesion or infiltration processes. The tidal-generated currents were relatively strong, reducing the likelihood of oil stranding or sediment deposition, particularly in Locations C2 and C1.

The validation results of the OS model with in-situ oil stranding amount measurements are shown in **Figure 7b**. The modeled amount values represent the average output every 5 min from when the oil entered the water until the end of the simulation. The R^2 coefficient value was 0.4636, with an RMSE of 1459.27. This correlation value indicates that 46.36% of the oil amount released by the model had a moderate correlation with the actual oil amount on the coast (Hair, 2011).

The physical, chemical, and biological interactions between oil and coastal sediments primarily influenced the OS model's accuracy. Although this suggests that our model has limited predictive capacity, in fact, many oil strandings are found on the west coast of Balikpapan Bay (see photos in **Figure 7c**). The model limitation was mainly due to the absence of sediment characteristics as a parameter in the modeling, as constrained by the technical settings in the 2013 version of the MIKE3 FM (Eco Lab/OS Module) software (DHI, 2013b). The current model parameters were limited using seabed roughness, coastal topography, waves, and tidal parameters. In the version of MIKE3 FM (Eco Lab/OS Module) software used in this research (DHI, 2013b), there were no numerical equations related to oil stranding to calculate oil concentration and its physical interaction with sediment characteristics. Meanwhile, including sediment material parameters is important in determining oil adhesion processes. Therefore, future research could benefit from using the latest MIKE Ecolab software (DHI, 2022), which has been updated to accommodate the physical processes of sedimentation components.

3.4. OS distribution in the water column (MIKE Model) and surface distribution Sentinel-1 SAR

Remote sensing data, such as Sentinel-1 SAR imagery, plays a crucial role in the rapid assessment and early detection of OS. However, understanding the behavior of OS distribution in the water column and seabed requires numerical modeling to complement surface observations. This section showed the results of the MIKE OS

model in the water column and the surface distribution OS derived from Sentinel-1 SAR to provide a comprehensive view of OS dynamics in Balikpapan Bay. Sentinel-1 SAR imagery captured on 1 April 2018, at 21:50 UTC, was re-processed following the method described by (Prastyani and Basith, 2018) to detect surface oil slicks. **Figure 8** presented overlay results between the OS in the surface detected by Sentinel-1 SAR imagery on 1 April 2018, at 21:50 UTC (**Figure 3**) and the modeled OS distribution in the water column from the coupled MIKE3 FM and MIKE OS module. The surface OS distribution from Sentinel-1 SAR indicates that the OS on the surface spanned 203.40 km^2, predominantly along the eastern coastline of the bay, extending toward the open sea into the Makassar Strait. Wind forcing played a significant role in the eastward drift of the surface oil, as corroborated by the wind patterns shown in **Figures 5e–f**.

In the water column, our results showed that the combined MIKE3 FM Hydrodynamic module and MIKE OS module were able to reproduce the subsurface (from the water column to seabed) layer distribution (timing and movement) of oil of Balikpapan Bay, which is a semi-enclosed water body with circulation patterns driven by tides, revealing a total exposure area of 137.52 km^2. In the case of the OS in Balikpapan Bay, with the spill source located at a depth of 28 m and in an area strongly influenced by tidal currents, a numerical modeling approach is essential for comprehensive interpretation. The OS model provided insight into the vertical and horizontal movement of oil in the sub-surface layer, which cannot be captured only by remote sensing data. In the subsurface layer, the OS model showed that the volume of oil was concentrated near the spill source and moved southward (toward the western coast of Balikpapan Bay) and inward to the bay, driven by tidal currents. At the same time, the satellite captured the oil slick movement along the eastern coast toward the Makassar Strait (**Figure 8**). In the transect C1 area (22 h and 33 min after the spill; see **Figure 1** or **Figure 7** for C1 location), oil in the water surface was quickly carried eastward due to wind and current dynamics. The predominant influence of wind force on the sea surface pushed oil flow eastward by the wind direction, as illustrated in **Figure 5e**,**f**). Simulations of wind-forcing results were significantly consistent with satellite observations, indicating that wind was the primary force driving oil dispersion in the surface water layer, as reported in previous studies (Cao et al., 2021; Gurumoorthi et al., 2021).

The combined analysis of surface and subsurface layers highlights the complementary roles of remote sensing and numerical modeling. Both approaches demonstrate the necessity of multi-source data for effective emergency response and environmental management of oil spills (OS). This study underscores the advantages of using remote sensing to detect surface oil dispersion and numerical modeling to understand subsurface dynamics, providing reliable estimates of oil distribution across different layers. These methods are particularly effective for mitigation and risk assessment of OS incidents in semi-enclosed water bodies like Balikpapan Bay.

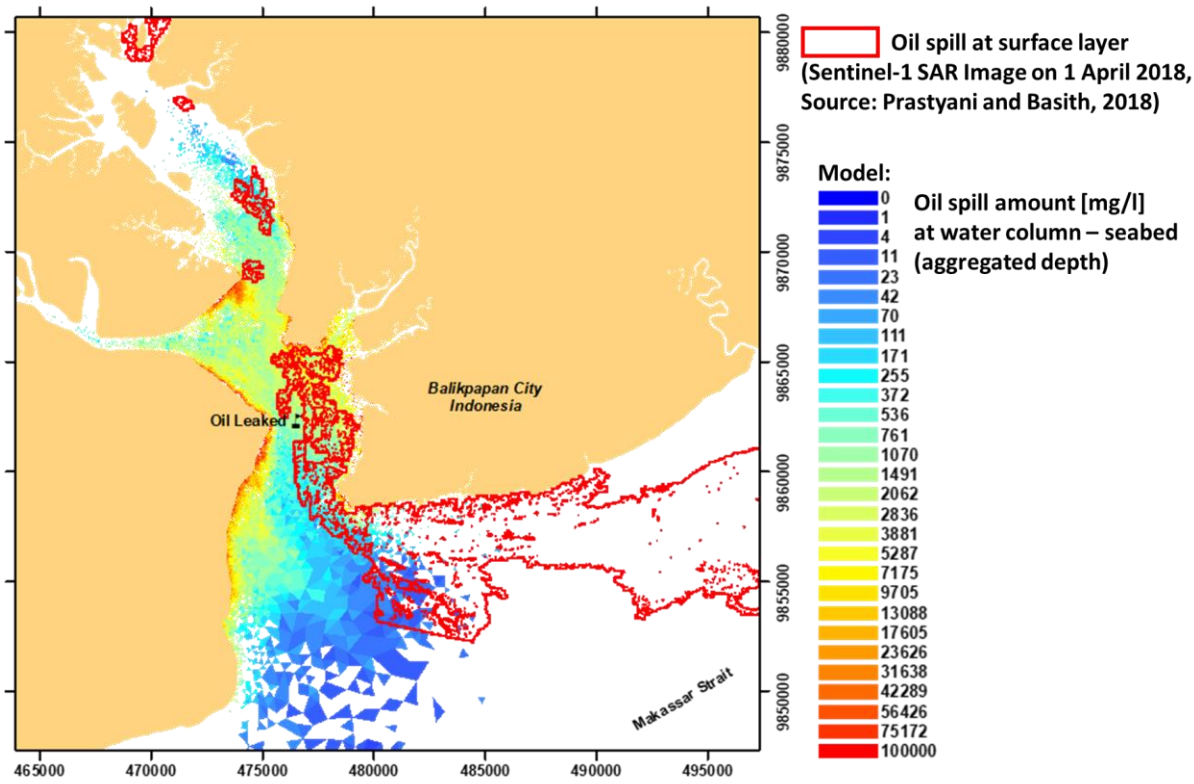

Figure 8. Composite of the oil slick observed by Sentinel-1 SAR image and oil amount distribution simulated by OS model dated on 1 April 2018, at 21:50 UTC. Sentinel-1 SAR detected an OS on the sea surface covering 203.40 km^2. The OS model measures 137.52 km^2. Both methods resulted in a synergistic OS exposure of 314.23 km^2.

4. Conclusions

This study effectively demonstrated the capabilities of the MIKE3 FM Hydrodynamic Module, coupled with the MIKE OS Module and in-situ observations, to generate a comprehensive crude OS model on water column into seabed for Balikpapan Bay. By integrating Sentinel-1 SAR data on oil slick distribution, the study provided a holistic view of the OS's behavior. The hydrodynamic (HD) model proved highly reliable in simulating water movements, with validation against tide (R^2 of 0.9179 of TD1 and 0.8848 of TD2) and current data (a gap of only 0.06 m/s), indicating the adequacy of the hydrodynamic model output from MIKE3 FM to serve as input for OS modeling yielding high correlation values. While Sentinel-1 SAR imagery captured surface oil slicks, the MIKE3 FM model simulated the OS distribution throughout the water column to the seabed.

The simulation results showed that oil from the leakage source spread 12.8 km seaward on day 1 and extended to 23.8 km by day 10.5, while within the bay, it progressed from 5.6 km on day 1 to 15.8 km on day 10.5. The area of oil-polluted waters increased from 98.96 km^2 on day 1 to 546.98 km^2 by day 10.5, a fivefold expansion. The highest oil amount on day 1 was recorded at the center of the bay (2495 mg/L), but by day 10.5, it had shifted to the western shore, reaching 65,277 mg/L. Oil trapped in beach sediments showed that Transect-3 had the highest amount (78,056 mg/kg), averaging 33,372 mg/kg. Validation of the OS model, which considered a depth-integrated (water column to seabed surface) layer, yielded an accuracy of

0.4636. However, the model lacked sediment characteristics in its parameterization due to limitations in the MIKE OS Module software version (2013).

The findings revealed that wind and tidal forces significantly influenced the dynamics of the OS, driving its spread both within the bay and out toward the Makassar Strait. The highest oil concentrations initially appeared in the bay's center but later shifted to the western shore. The model also detected oil trapped in coastal sediments, which could not be observed using satellite imagery alone. While the OS model showed near-even OS distribution throughout the bay, the Sentinel-1 SAR imagery predominantly detected surface oil, driven by wind forces eastward, covering an area of 203.40 km^2.

Despite the model's effectiveness, several limitations were identified, particularly the absence of sediment parameterization, wave impacts, and biological interactions in the oil stranding process. Future research should address these factors to improve the accuracy of OS simulations and better understand their environmental impacts.

In conclusion, the combined use of 3D numerical modeling and satellite observations offers a robust framework for OS disaster mitigation and environmental management, underscoring the need for a comprehensive, multi-layered analysis in semi-enclosed water body like Balikpapan Bay.

Supplementary materials: Supplementary materials to this article can be found online at https://doi.org/10.24294/jipd10173XXX.

Author contributions: Conceptualization, AP, WA, IWN, and RA; methodology, AP and IWN; software, YA and DN; validation, AWR, EP and MH; formal analysis, AP, IWN, and RA; investigation, RA, YSD, EP, MH, and SB; resources, DN; data curation, RA, AWR, and SB; writing—original draft preparation, AP, WA, and AWR; writing—review and editing, IWN, WW, and YSD; visualization, YA, DN and SB; supervision, WW; project administration, RA; funding acquisition, RA. All authors have read and agreed to the published version of the manuscript.

Funding: This work was supported by PT Pertamina (Persero), Indonesia under project title "Penentuan Area Terdampak dan Perhitungan Kerugian Akibat Tumpahan Minyak di Teluk Balikpapan (Determination of Affected Areas and Calculation of Losses due to OS in Balikpapan Bay)", Grant number 026/E15000/2018-S0, December 2018 and executed by the Institute of Research and Community Empowerment of IPB University.

Acknowledgments: The authors thank PT PERTAMINA (Persero) Indonesia for the financial support of this research. Besides, we acknowledge the Institute of Research and Community Empowerment of IPB University and the National Research and Innovation Agency (BRIN) for conducting and supporting the research. Lastly, thanks to the reviewers for their work in improving the quality of this manuscript.

Conflict of interest: The authors declare no conflict of interest.

References

Apiratikul, R., Pongpiachan, S., and Hashmi, M. Z. (2020). Health risk assessment of polycyclic aromatic hydrocarbons in coastal soils of Koh Samed Island (Thailand) after the oil spill incident in 2013. Marine Pollution Bulletin, 150, 110736. https://doi.org/10.1016/J.MARPOLBUL.2019.110736

Barreto, F. T. C., Dammann, D. O., Tessarolo, L. F., Skancke, J., Keghouche, I., Innocentini, V., Winther-Kaland, N., and Marton, L. (2021). Comparison of the Coupled Model for Oil spill Prediction (CMOP) and the Oil Spill Contingency and Response model (OSCAR) during the DeepSpill field experiment. Ocean & Coastal Management, 204, 105552. https://doi.org/10.1016/J.OCECOAMAN.2021.105552

Bejarano, A. C., Adams, J. E., McDowell, J., Parkerton, T. F., and Hanson, M. L. (2023). Recommendations for improving the reporting and communication of aquatic toxicity studies for oil spill planning, response, and environmental assessment. Aquatic Toxicology, 255, 106391. https://doi.org/10.1016/J.AQUATOX.2022.106391

Cao, Y., Zhang, B., Zhu, Z., Rostami, M., Dong, G., Ling, J., Lee, K., Greer, C. W., and Chen, B. (2021). Access-dispersion-recovery strategy for enhanced mitigation of heavy crude oil pollution using magnetic nanoparticles decorated bacteria. Bioresource Technology, 337, 125404. https://doi.org/https://doi.org/10.1016/j.biortech.2021.125404

Cheng, L., Li, Y., Qin, M., and Liu, B. (2024). A marine oil spill detection framework considering special disturbances using Sentinel-1 data in the Suez Canal. Marine Pollution Bulletin, 208(May), 117012. https://doi.org/10.1016/j.marpolbul.2024.117012

Daly, K. L., Remsen, A., Outram, D. M., Broadbent, H., Kramer, K., and Dubickas, K. (2021). Resilience of the zooplankton community in the northeast Gulf of Mexico during and after the Deepwater Horizon oil spill. Marine Pollution Bulletin, 163, 111882. https://doi.org/10.1016/j.marpolbul.2020.111882

De Padova, D., Mossa, M., Adamo, M., De Carolis, G., and Pasquariello, G. (2017). Synergistic use of an oil drift model and remote sensing observations for oil spill monitoring. Environmental Science and Pollution Research, 24(6), 5530–5543. https://doi.org/10.1007/s11356-016-8214-8

DHI. (2013a). MIKE 21 & MIKE 3 Flow Model FM (Hydrodynamic and Transport Module).

DHI. (2013b). MIKE 3 FLOW MODEL FM (ECO Lab / Oil Spill Module).

DHI. (2014a). DHI Oil Spill Model (Oil Spill Template Scientific Documentation). www.mikepoweredbydhi.com

DHI. (2014b). MIKE 3 FLOW MODEL Hydrostatic Version.

DHI. (2022). MIKE ECO Lab Scientific.

Fingas, M., and Brown, C. (2014). Review of oil spill remote sensing. Marine Pollution Bulletin, 83(1), 9–23. https://doi.org/10.1016/j.marpolbul.2014.03.059

Fingas, M., and Brown, C. E. (2017). Oil Spill Remote Sensing. In Oil Spill Science and Technology: Second Edition (pp. 305–385). Elsevier Inc. https://doi.org/10.1016/B978-0-12-809413-6.00005-9

French-McCay, D. P., Jayko, K., Li, Z., Spaulding, M. L., Crowley, D., Mendelsohn, D., Horn, M., Isaji, T., Kim, Y. H., Fontenault, J., and Rowe, J. J. (2021). Oil fate and mass balance for the Deepwater Horizon oil spill. Marine Pollution Bulletin, 171, 112681. https://doi.org/10.1016/j.marpolbul.2021.112681

Gao, Y., Li, F., Mao, L., Yan, N., Peng, C., Tao, H., and Zhang, D. (2022). Simulation on water quality of reservoir at construction phase by pollutant release from oxidation of waste rocks rich S and Fe. Environmental Technology and Innovation, 28(516), 102860. https://doi.org/10.1016/j.eti.2022.102860

Guan, X., Ma, J., Huang, J., Huang, R., Zhang, L., and Ma, Z. (2019). Impact of oceans on climate change in drylands. Science China Earth Sciences, 62(6), 891–908. https://doi.org/10.1007/s11430-018-9317-8

Gurumoorthi, K., Suneel, V., Trinadha Rao, V., Thomas, A. P., and Alex, M. J. (2021). Fate of MV Wakashio oil spill off Mauritius coast through modelling and remote sensing observations. Marine Pollution Bulletin, 172(August), 112892. https://doi.org/10.1016/j.marpolbul.2021.112892

Hair, J. F. (2011). Multivariate Data Analysis (Fifth Edit). PrenticeHall Inc.

Hidayat, R., Sartimbul, A., and Wibowo, M. (2021). Simulation of Oil Spill Pollution due to Tsunami in Cilacap, Central Java, Indonesia. International Journal on Advanced Science Engineering and Information Technology, 11(3). https://doi.org/10.18517/ijaseit.11.3.14264

Hong, J. H., Semprucci, F., Jeong, R., Kim, K., Lee, S., Jeon, D., Yoo, H., Kim, J., Kim, J., Yeom, J., Lee, S., Lee, K., and Lee, W. (2020). Meiobenthic nematodes in the assessment of the relative impact of human activities on coastal marine ecosystem. Environmental Monitoring and Assessment, 192(2), 1–13. https://doi.org/10.1007/S10661-019-8055-2/TABLES/2

Huang, K., Nie, W., and Luo, N. (2020). Scenario-Based Marine Oil Spill Emergency Response Using Hybrid Deep Reinforcement Learning and Case-Based Reasoning. Applied Sciences 2020, Vol. 10, Page 5269, 10(15), 5269. https://doi.org/10.3390/APP10155269

Khoi, D. N., Nguyen, V. T., Loi, P. T., Hong, N. V., Thuy, N. T. D. D., and Linh, D. Q. (2023). Development of an integrated tool responding to accidental oil spills in riverine and shoreline areas of Ho Chi Minh City, Vietnam. Environmental Impact Assessment Review, 99(December 2022), 106987. https://doi.org/10.1016/j.eiar.2022.106987

Lahjie, A. M., Nouval, B., Lahjie, A. A., Ruslim, Y., and Kristiningrum, R. (2019). Economic valuation from direct use of mangrove forest restoration in Balikpapan Bay, East Kalimantan, Indonesia. F1000Research, 8, 1–13. https://doi.org/10.12688/f1000research.17012.2

Li, C., Kim, D. jin, Park, S., Kim, J., and Song, J. (2023). A self-evolving deep learning algorithm for automatic oil spill detection in Sentinel-1 SAR images. Remote Sensing of Environment, 299(October), 113872. https://doi.org/10.1016/j.rse.2023.113872

Liu, Z., and Callies, U. (2019). Implications of using chemical dispersants to combat oil spills in the German Bight – Depiction by means of a Bayesian network. Environmental Pollution, 248, 609–620. https://doi.org/10.1016/J.ENVPOL.2019.02.063

Liu, Z., Chen, Q., Zheng, C., Han, Z., Cai, B., and Liu, Y. (2022). Oil spill modeling of Chengdao oilfield in the Chinese Bohai Sea. Ocean Engineering, 255(April), 111422. https://doi.org/10.1016/j.oceaneng.2022.111422

Melillos, G., and Hadjimitsis, D. G. (2021). Oil spill detection using sentinel 1 SAR data at Cyprus's coasts. Https://Doi.Org/10.1117/12.2585886, 11729(April), 19. https://doi.org/10.1117/12.2585886

Motorin, D., Roozbahani, H., and Handroos, H. (2022). Development of a novel method for estimating and planning automatic skimmer operation in response to offshore oil spills. Journal of Environmental Management, 318(March), 115451. https://doi.org/10.1016/j.jenvman.2022.115451

Muin, M., Muslim, A. B., and Puspitasari, T. A. (2022). The Effect of Non-Linear Wave on Oil Spill Dispersion. IOP Conference Series: Earth and Environmental Science, 1065(1). https://doi.org/10.1088/1755-1315/1065/1/012006

Nixon, Z., and Michel, J. (2018). A Review of distribution and quantity of lingering subsurface oil from the Exxon Valdez Oil Spill. Deep-Sea Research Part II: Topical Studies in Oceanography, 147(July 2017), 20–26. https://doi.org/10.1016/j.dsr2.2017.07.009

Owens, E. H., Taylor, E., and Humphrey, B. (2008). The persistence and character of stranded oil on coarse-sediment beaches. Marine Pollution Bulletin, 56(1), 14–26. https://doi.org/10.1016/j.marpolbul.2007.08.020

Prastyani, R., and Basith, A. (2018). Utilisation of Sentinel-1 SAR Imagery for Oil Spill Mapping: A Case Study of Balikpapan Bay Oil Spill. JGISE: Journal of Geospatial Information Science and Engineering, 1(1), 22–26. https://doi.org/10.22146/jgise.38533

Rajendran, S., Vethamony, P., Sadooni, F. N., Al-Kuwari, H. A. S., Al-Khayat, J. A., Govil, H., and Nasir, S. (2021). Sentinel-2 image transformation methods for mapping oil spill – A case study with Wakashio oil spill in the Indian Ocean, off Mauritius. MethodsX, 8. https://doi.org/10.1016/j.mex.2021.101327

Rajendran, S., Vethamony, P., Sadooni, F. N., Al-Kuwari, H. A. S., Al-Khayat, J. A., Seegobin, V. O., Govil, H., and Nasir, S. (2021). Detection of Wakashio oil spill off Mauritius using Sentinel-1 and 2 data: Capability of sensors, image transformation methods and mapping. Environmental Pollution, 274, 116618. https://doi.org/10.1016/j.envpol.2021.116618

Rana, F. M., Adamo, M., Lucas, R., and Blonda, P. (2019). Sea surface wind retrieval in coastal areas by means of Sentinel-1 and numerical weather prediction model data. Remote Sensing of Environment, 225(March), 379–391. https://doi.org/10.1016/j.rse.2019.03.019

Spies, R. B., Mukhtasor, M., and Burns, K. A. (2017). The Montara Oil Spill: A 2009 Well Blowout in the Timor Sea. Archives of Environmental Contamination and Toxicology, 73(1), 55–62. https://doi.org/10.1007/S00244-016-0356-7/FIGURES/5

Sulma, S., Insan Nur Rahmi, K., Febrianti, N., and Sitorus, J. (2019). DETEKSI TUMPAHAN MINYAK MENGGUNAKAN METODE ADAPTIVE THRESHOLD DAN ANALISIS TEKSTUR PADA DATA SAR (Oil Spill Detection using Adaptive Threshold and Texture Analysis Methode on SAR Data). Majalah Ilmiah Globe, 21(1), 45–52. https://doi.org/10.24895/MIG.2019.25-1.925

Wang, C., Chen, B., Zhang, B., He, S., and Zhao, M. (2013). Fingerprint and weathering characteristics of crude oils after Dalian oil spill, China. Marine Pollution Bulletin, 71(1–2), 64–68. https://doi.org/10.1016/J.MARPOLBUL.2013.03.034

Weiskopf, S. R., Rubenstein, M. A., Crozier, L. G., Gaichas, S., Griffis, R., Halofsky, J. E., Hyde, K. J. W., Morelli, T. L., Morisette, J. T., Muñoz, R. C., Pershing, A. J., Peterson, D. L., Poudel, R., Staudinger, M. D., Sutton-Grier, A. E., Thompson, L., Vose, J., Weltzin, J. F., and Whyte, K. P. (2020). Climate change effects on biodiversity, ecosystems, ecosystem services, and natural resource management in the United States. Science of the Total Environment, 733. https://doi.org/10.1016/j.scitotenv.2020.137782

Zu, T., and Gan, J. (2009). PROCESS-ORIENTED STUDY OF THE RIVER PLUME AND CIRCULATION IN THE PEARL RIVER ESTUARY: RESPONSE TO THE WIND AND TIDAL FORCING. In Advances in Geosciences (pp. 213–230). https://doi.org/10.1142/9789812836168_0015